

Two-dimensional magneto-optical trap as a source of slow atoms

K. Dieckmann,¹ R. J. C. Spreeuw,² M. Weidemüller,^{1,*} and J. T. M. Walraven¹

¹*FOM–Institute for Atomic and Molecular Physics, Kruislaan 407, 1098 SJ Amsterdam, The Netherlands*

²*Van der Waals–Zeeman Institute, Valckenierstraat 65-67, 1018 XE Amsterdam, The Netherlands*

(Received 2 July 1998)

We experimentally study the use of two-dimensional magneto-optical trapping (2D-MOT) for the generation of slow beams of cold atoms out of a vapor cell. A particularly high flux of 9×10^9 rubidium atoms/s at a mean velocity of 8 m/s is obtained using a combination of magneto-optical trapping in two dimensions and Doppler cooling in the third dimension (2D⁺-MOT). The resulting width of the velocity distribution is 3.3 m/s [full width at half maximum (FWHM)] with a beam divergence of 43 mrad (FWHM). We investigate the total flux as a function of vapor cell pressure and determine the velocity distribution of our slow atom sources. For comparison, we also realized a low-velocity intense source (LVIS), first reported by Lu *et al.* [Phys. Rev. Lett. **77**, 3331 (1996)]. We find that the 2D⁺-MOT yields a significantly higher flux than the LVIS, even when used with an order of magnitude less laser power. [S1050-2947(98)04311-X]

PACS number(s): 32.80.Pj, 42.50.Vk, 03.75.-b

I. INTRODUCTION

Optical cooling and trapping in two dimensions have been applied successfully to the brightening of fast atomic beams [1–3]. The atomic beam is compressed and the atomic motion cooled in the two directions transverse to the beam axis. This two-dimensional cooling principle has been called an ‘‘atomic funnel,’’ or also a two-dimensional magneto-optical trap (2D-MOT). It is less well established that two-dimensional cooling, besides the *brightening* of atom beams, is also a powerful technique for the *generation* of slow (< 30 m/s) atom beams. The generation of intense sources of slow atomic beams is of great interest for experiments on Bose-Einstein condensation [4–6]. One of the earliest and most widely used techniques is to slow down atoms from a thermal oven using the Zeeman-slowness technique [7]. More recently there have been efforts to use optical cooling techniques to extract slow atomic beams from low-pressure vapor cells. The most intense source of this kind so far, the so-called low-velocity intense source (LVIS) [8], is based on three-dimensional cooling.

In this paper we study two-dimensional cooling configurations which extract a beam of slow atoms directly out of a vapor cell. Although a two-dimensional cooling configuration seems an obvious geometrical choice for beam generation, experimental work has been limited. A two-dimensional technique achieving a relatively low flux of slow atoms has been demonstrated recently by Weyers *et al.* [9]. A similar method to generate a very slow beam was recently described by Berthoud *et al.* [10]. We report here the experimental realization of two vapor-cell based sources for a slow and intense atomic beam, based on two-dimensional trapping and cooling. Our brightest source is based on a combination of a 2D-MOT and unbalanced optical molasses in the third, longitudinal direction (2D⁺-MOT configuration). It yields a flux of slow atoms comparable to the LVIS [8], but requires

an order of magnitude less laser power than employed in the original realization of the LVIS. We realized the LVIS with low laser power, so that we can compare the performance of the sources directly.

II. EXPERIMENTAL SETUP AND PRINCIPLE OF OPERATION

The experimental setup is based on a two-chamber vacuum system. A rubidium vapor cell is formed by a rectangular quartz cuvette ($30 \times 30 \times 150$ mm³). The vapor pressure is varied between a few 10^{-9} mbar and 5×10^{-7} mbar by heating a rubidium reservoir connected to the vapor cell. The vapor pressure is measured with a calibrated photodiode detecting the fluorescence induced by a laser beam of 1.4 mW power and 7 mm waist. The atom beam leaves the vapor cell in the upward vertical direction through a 0.8 mm diameter hole. It then enters an ultrahigh vacuum chamber where it is analyzed. The small hole at the same time allows for differential pumping.

The principal part of our experimental setup around the vacuum system is shown in Fig. 1. Two sets of coils placed around the vapor cell are used to produce the desired inhomogeneous magnetic fields. A set of four racetrack-shaped coils generates a cylindrical quadrupole field with a line of zero magnetic field along the symmetry axis. This quadrupole field is used for the 2D-MOT and 2D⁺-MOT configurations. A pair of anti-Helmholtz coils generates a spherical quadrupole field used in the LVIS.

The laser system consists of 50 mW diode lasers which are linewidth-narrowed by optical feedback from an external grating and frequency-stabilized by electronic feedback from Doppler-free saturated absorption spectroscopy in a Rb cell. The first, ‘‘cooling and trapping,’’ laser is tuned a few linewidths to the red of the $5S_{1/2} (F=2) \rightarrow 5P_{3/2} (F=3)$ transition in ⁸⁷Rb. This laser acts as a master, to which another low power diode laser is slaved by injection locking, yielding a power of 34 mW filtered into a TEM₀₀ mode. The second, ‘‘repumping,’’ laser is resonant with the $5S_{1/2} (F=1) \rightarrow 5P_{3/2} (F=2)$ transition and is used for hyperfine repumping. The lasers and field coils are used in three different

*Present address: Max-Planck-Institut für Kernphysik, Saupfercheckweg 1, D-69117 Heidelberg, Germany.

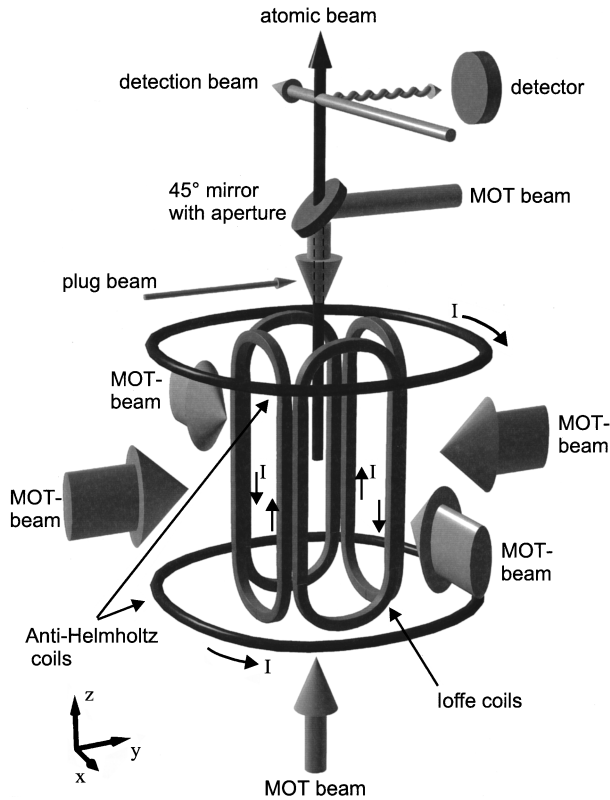


FIG. 1. Experimental setup: The rubidium vapor cell from which the atomic beam is extracted is located inside the four racetrack-shaped magnetic field coils. These so-called Ioffe coils produce a two-dimensional quadrupolar magnetic field and are used in the 2D-MOT and 2D⁺-MOT configurations. The anti-Helmholtz coils are used for the three-dimensional quadrupolar field necessary for the 2D⁺-MOT and the LVIS configuration. The vertical MOT beams used for the 2D⁺-MOT and the LVIS are absent in the 2D-MOT case. After passing through an aperture in a 45° mirror into an ultrahigh vacuum chamber, the atomic beam is detected by means of fluorescence.

combinations (2D-MOT, 2D⁺-MOT, and LVIS), using the experimental parameters listed in Table I.

For the 2D-MOT we use two pairs of retroreflected cooling beams ($\sigma^+ - \sigma^-$ polarization). These beam pairs are perpendicular to each other and to the atomic beam axis, defined by the (vertical) line of zero magnetic field of the cylindrical quadrupole coils. The laser beams have an elliptical cross section, with the larger waist $w_z = 24$ mm along the atomic beam axis and the smaller waist $w_\rho = 7$ mm perpendicular to it. Rubidium atoms from the background vapor passing through the cooling fields are cooled and driven towards the symmetry axis. Their velocity component v_z along the axis is conserved, since all cooling beams exclusively propagate in the horizontal plane. From this two-dimensional version of the magneto-optical trap (2D-MOT) two atomic beams emerge upwards and downwards, respectively, along the symmetry axis. Atoms with a high longitudinal velocity v_z do not spend enough time in the laser fields to be sufficiently cooled in the transverse direction. These atoms are filtered out by the 0.8 mm aperture. Because of this “filtering” for short interaction times, the longitudinal velocity of atoms in the beam is small compared to the average velocity of atoms in the background of 270 m/s.

TABLE I. Experimental parameters of the three source configurations: Laser detuning is given in units of the natural linewidth ($\Gamma \approx 2\pi \times 6$ MHz). Magnetic field gradient and waist (radius at $1/e^2$ fraction of peak intensity) as well as power of the laser beams refer to the vertical (z, \uparrow, \downarrow) and horizontal (ρ, \leftrightarrow) direction.

	2D-MOT	2D ⁺ -MOT	LVIS
Detuning δ	-1.7Γ	-3Γ	-3.3Γ
Field gradient:			
dB/dz (G/cm)	0	0	13.6
$dB/d\rho$ (G/cm)	17.7	12.6	6.8
Laser waists:			
w_ρ (mm)	7	7	7
w_z (mm)	24	24	7
Laser power:			
P_\downarrow (mW):	0	0.64	3.8
P_\uparrow (mW):	0	2.1	5.2
P_{\leftrightarrow} (mW):	16.4	15	10.4

The 2D⁺-MOT is an extension of the 2D-MOT, where we apply an additional pair of laser beams in the vertical (z) direction. The extra pair of beams cools the axial velocity v_z and thus enhances the capture of atoms with a large v_z . The intensities of the two vertical beams are adjusted independently. The highest atomic flux is found if the upward propagating beam is more intense than the downward one, so that radiation pressure is unbalanced, pushing the atoms upwards through the 0.8 mm hole. We used 0.6 mW of power in the downward beam and 2.1 mW in the upward beam, both beams having a waist of 7 mm. Furthermore, the downward propagating beam enters the vacuum from the side and is reflected downward by a 45° aluminum mirror, in the center of which the 0.8 mm exit hole is drilled. Therefore the downward propagating beam contains a shadow along the axis so that atoms close to the axis are strongly accelerated out of the capture region by the upward propagating beam. We would like to notice here that the two vertical laser beams have equal detunings as the transverse beams. A separate detuning of the vertical beams could lead to an enhanced axial capture velocity and thus a higher atomic flux.

For the LVIS, six intensity-balanced circularly polarized laser beams are combined with the spherical quadrupole field of the anti-Helmholtz coils. Also in the LVIS the downward propagating beam contains a shadow along the axis and atoms are driven out of the capture region by radiation pressure from the upward propagating beam. All laser beams have a circular cross section with a 7 mm waist, limited by the available laser power. Due to this relatively small waist, the optimum magnetic field gradient is relatively large, $dB/dz = 15$ G/cm, about a factor 3 larger than in the original experiment by Lu *et al.* [8].

III. DIAGNOSTICS

The resulting cold atom beams are analyzed by detecting the fluorescence from a resonant probe laser beam located 130 mm above the exit hole. The probe has a power of 1 mW and a waist of 0.3 mm. A second, overlapping, beam with a power of 80 μ W is used for hyperfine repumping. The fluorescence is measured using a calibrated photomultiplier tube

(Hamamatsu 928). The photomultiplier signal is a measure for the local density of atoms passing through the probe beam. By translating the position of the narrow detection beam, the transverse density profile of the atomic beam can be resolved, and thus the divergence can be determined.

The longitudinal velocity distribution of the atomic beam is measured using a time-of-flight method, by suddenly switching off the atomic beam. This is accomplished by switching on an additional resonant “plug” laser beam that pushes the atoms away from the axis before they reach the exit aperture. From the time dependence of the decaying fluorescence signal $S(\tau)$ after switching off the atomic beam, the longitudinal velocity distribution $\Phi(v)$ can be deduced. Since the atom beam propagates vertically, the velocity distribution changes under the influence of gravity. The velocity distribution of the atom flux at the position of the plug beam is given by

$$\Phi(v) = -\frac{\tau}{\eta} \frac{dS(\tau)}{d\tau} \quad \text{with} \quad v = \frac{L}{\tau} + \frac{g\tau}{2}. \quad (1)$$

Here η is a calibration factor of the detection system, $L = 135$ mm is the distance between the plug and detection beams, and g is the acceleration due to gravity. The integral $\int \Phi(v) dv$ gives the total flux in atoms/s.

IV. BEAM PROFILES AND VELOCITY DISTRIBUTIONS

The measured transverse density profiles of the atomic beams can well be fitted by a Gaussian. In the 2D-MOT and the 2D⁺-MOT we observe atomic beam divergences of 46 mrad and 43 mrad (FWHM), respectively. In the LVIS we find a smaller beam divergence of 27 mrad (FWHM). In all cases the value of the beam divergence seems to be limited geometrically by the angle subtended by the 0.8 mm exit hole as seen from the trapping region. Note that in our apparatus the distance from the edge of the trapping region to the exit hole is the same for the 2D-MOT and 2D⁺-MOT, but about twice as large for the LVIS, as we use different waists for the transverse laser beams (Table I).

The measured velocity distributions of the flux $\Phi(v)$ at the level of the plug beam are shown in Fig. 2. For the 2D⁺-MOT and LVIS the distributions are close to Gaussian, centered at a nonzero value. These distributions are determined by the *longitudinal* cooling process and subsequent acceleration out of the trapping region, by radiation pressure. There is a striking difference in average velocity—the mean value of the distribution $\Phi(v)$ —between the beams produced by the 2D⁺-MOT (8 m/s) and LVIS (26 m/s). This is due to the different intensities of the upwards propagating beams used in both cases, by which the atoms are accelerated out of the trapping region (Table I). In both cases we observe a slight decrease of the mean velocity with increasing vapor pressure. If the pressure is increased, the atomic beam becomes optically dense. Thus, the radiation pressure from the upward propagating beam is reduced, which accelerates the atoms traveling in the shadow of the downward propagating beam. The widths (FWHM) of the velocity distributions of the 2D⁺-MOT and the LVIS are 3.3 m/s and 6.3 m/s. As the radiation pressure accelerating the atomic beam is higher in case of the LVIS, the velocity distribution of the LVIS is

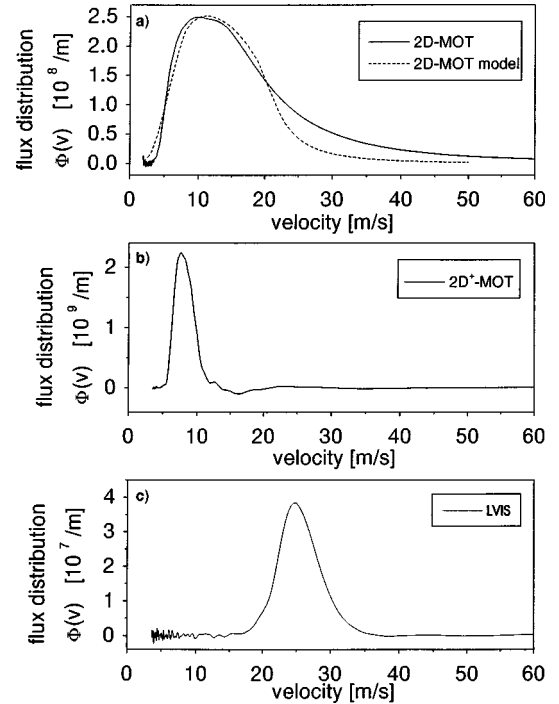


FIG. 2. Velocity distributions $\Phi(v)$ of the flux. (a) Comparison of 2D-MOT and our simple model, (b) 2D⁺-MOT, (c) LVIS. The data are obtained by taking the derivative of the time-resolved photomultiplier signal [Eq. (1)]. The curves were measured at different background pressure in order to optimize the respective flux [Fig. 3(a)]. The small dip towards negative flux in (b) around $v = 17$ m/s is an artifact resulting from a fluctuation of the time-of-flight signal.

broader than that of the 2D⁺-MOT. In both cases we observe a reduction of the width of the velocity distributions with increasing pressure, i.e., with decreasing radiation pressure.

The flux distribution of the 2D-MOT is entirely different, because in this case there is neither longitudinal cooling nor an acceleration out of the trapping region. The velocity distribution here is determined by the *transverse* rather than the longitudinal cooling process. The basic features of the distribution are reproduced by a simple transverse cooling model, as will be discussed below.

V. TOTAL FLUX AND INFLUENCE OF COLLISIONS

The total flux of each of the three atomic beam sources has been measured as a function of the rubidium vapor pressure. The pressure was varied up to the saturated vapor pressure at room temperature of about 4.8×10^{-7} mbar. The results are shown in Fig. 3(a). In the absence of collisions the total flux should be proportional to the rubidium pressure. In all three cases this is indeed observed at low vapor pressure. In this regime the LVIS configuration produces a higher atomic flux than the 2D-MOT and 2D⁺-MOT. The LVIS works more efficiently because of the presence of an optical confinement in all three directions. Atoms in the beam which do not travel collinear with the shadow of the downwards propagating beam enter the light field again. Due to the restoring force in all directions these atoms will be driven to the center again. Because of this *recycling* effect, almost all atoms, once captured, eventually are extracted via the exit hole [8]. By contrast, such atoms in the beam which do not

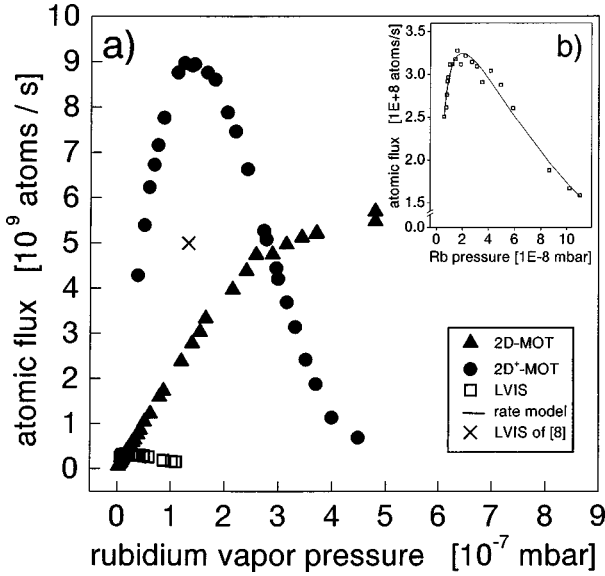


FIG. 3. Flux of the atomic beam versus rubidium vapor pressure: (a) Comparison between the three experimental configurations. At low vapor pressure the flux increases linearly with the density in the background vapor. The flux of the $2D^+$ -MOT configuration generated by means of 34-mW laser power exceeds that of the original LVIS [8], using 500 mW. (b) Comparison of the measured pressure dependence of the LVIS flux with a simple rate model described by Eq. (2).

pass through the exit hole are lost in the 2D-MOT and $2D^+$ -MOT cases.

At higher vapor pressure the measured curves deviate from a linear relationship. This shows that collisions play a very important role in both the $2D^+$ -MOT and the LVIS, causing the total flux to decrease as the pressure exceeds an optimum value. The LVIS reaches its maximum flux of 3×10^7 atoms/s at a vapor pressure of 2×10^{-8} mbar. The $2D^+$ -MOT reaches its maximum flux of 9×10^9 atoms/s at a vapor pressure of 1.5×10^{-7} mbar. This flux is comparable to the original LVIS source reported by Lu *et al.* [8], but requires an order of magnitude less laser power. Thus, for a given laser power and optimized vapor pressure, the flux from the $2D^+$ -MOT surpasses the one from the LVIS.

In the 2D-MOT collisions play only a minor role. The deviation from linearity is small, and the flux steadily increases even at the saturated vapor pressure. This marked difference is probably due to the absence of a pushing laser beam for the extraction of the atoms. The atoms that leave the 2D-MOT no longer interact with the laser beam. In the $2D^+$ -MOT and LVIS, on the other hand, the extracted atoms are in the light field of the extraction laser beam. It is well known that collisions in the presence of near-resonant light can have a very large cross section [11], due to the strong resonant dipole-dipole interaction, described by a C_3/R^3 potential. Another reason why the 2D-MOT should be less affected by collisions is that the atoms spend a shorter time in the light field because their longitudinal velocity is left unchanged.

In order to include the effect of collisional loss in the extracted beam of the LVIS, we extend the simple rate model for the atomic flux Φ given in [8]:

$$\Phi = \frac{R}{1 + \Gamma_{\text{trap}}/\Gamma_{\text{out}}} \exp(-\Gamma_{\text{beam}} t_{\text{out}}). \quad (2)$$

In this equation R is the rate at which the trap captures atoms out of the background vapor, Γ_{trap} is the loss rate out of the trap due to background collisions, and Γ_{out} is the constant outcoupling rate of atoms from the cloud into the beam. Both R and Γ_{trap} are proportional to the background rubidium density n_{Rb} . The extension here is the inclusion of an exponential loss factor $\exp(-\Gamma_{\text{beam}} t_{\text{out}})$. It represents the decay of the flux due to background collisions as the atoms travel towards the exit hole with rate $\Gamma_{\text{beam}} \propto n_{\text{Rb}}$, during a time $t_{\text{out}} \approx 1$ ms. By fitting Eq. (2) to our LVIS data, as shown in Fig. 3(b), we determine the effective collision cross section for loss out of the beam, $\sigma_{\text{eff}} = \Gamma_{\text{beam}} / n_{\text{Rb}} \bar{v} = 2.3 \times 10^{-12}$ cm², with $\bar{v} = 270$ m/s the average thermal velocity of the background Rb.

This value agrees well with a calculation assuming that atoms in the beam interact with background Rb atoms through a C_3/R^3 potential (resonant dipole-dipole interaction). Adapting the approach described in [12] for loss out of a beam rather than a 3D trap, we find

$$\sigma_{\text{eff}} = 6.52 \left(\frac{C_3}{m v_{\text{esc}} \bar{v}} \right)^{2/3} \approx 3 \times 10^{-12} \text{ cm}^2. \quad (3)$$

Here m is the mass of a ^{87}Rb atom and the escape velocity $v_{\text{esc}} \approx 0.4$ m/s is the estimated transverse velocity kick needed to make an atom miss the exit hole.

VI. MODEL FOR THE 2D-MOT

The velocity distribution of the flux as well as the total flux of the 2D-MOT can be understood from a simple model of the transverse cooling process. The model uses a number of simplifications. The atomic transition is approximated by taking a $J=0$ ground state and $J'=1$ excited state with Landé g factor $g=1$. For the light force we take simply the sum of two spontaneous scattering forces from a counter-propagating beam pair, accounting for Zeeman and Doppler shifts. It has been argued by Lindquist *et al.* [13] that saturation effects in an inhomogeneous magnetic field can be neglected, because one beam of each counterpropagating pair is always closer to resonance.

The resulting force depends only on the combination $x + v_x \tau$ of horizontal position x and velocity v_x , where $\tau = 0.5$ ms is a characteristic time constant. This force is linearized around $x + v_x \tau = 0$ and truncated: $F(x + v_x \tau) = 0$ if $|x + v_x \tau| > x_c = 8$ mm. The resulting damped harmonic oscillator is underdamped for our experimental conditions, with oscillation frequency $\omega/2\pi = 310$ Hz and damping rate $\gamma/2\pi = 266$ Hz. The spatial profile of the laser beams is ignored, assuming a uniform intensity inside the beams and zero outside.

Atoms enter the cooling region according to a Maxwell-Boltzmann distribution. They enter the cooling region either transversely or longitudinally (“funneling”). We take the axial velocity v_z as a conserved quantity. The transverse motion of an atom that enters the light field at position z is cooled during a transit time $(l-z)/v_z$, with l the position

where the light field ends. After the atom leaves the light field at $z=l$ with transverse position and velocity (x, v_x) , it may traverse to the exit hole, at $z=l+h$, during a time h/v_z . The atom can exit through the hole if $|x+v_x h/v_z| < R_h$, where R_h is the radius of the hole.

The velocity distribution resulting from this model is shown in Fig. 2(a). Based on the model we find that the velocity distribution of the 2D-MOT flux is determined by three main processes. First, the main share of slow atoms, with velocity lower than about 20 m/s, results from transverse capture. Atoms enter the light field in a direction transverse to the axis, their transverse motion is damped and they leave along the axis. Atoms that are faster than about 20 m/s spend insufficient time in the light field for the transverse cooling to be effective. The value of 20 m/s thus depends on the spatial extent of the laser fields along the axis of the transverse laser beams. Second, the tail of relatively fast atoms, ≈ 20 m/s, is due to ‘‘funneling,’’ i.e., atoms that enter the light field in the longitudinal direction, through the end cap of the cylindrical cooling region. Third, the absence of atoms at very low velocity is due to the finite transverse temperature reached by the 2D cooling field. The distance between the light field and the exit hole is about 20 mm. As the atoms traverse this distance, their finite transverse velocity leads them astray from the axis. As the corresponding beam divergence is comparatively high for slow atoms in the longitudinal direction, slow atoms are filtered from the beam by the exit aperture.

The model predicts that collisional loss is essentially unimportant in the 2D-MOT as long as the rubidium pressure in the vapor cell is below about 2×10^{-7} mbar. Below this value, the total flux grows linearly with the rubidium pressure. If the pressure is further increased, collisions cause the total flux to grow slower than linear. The model predicts that at even higher vapor pressure the flux will eventually decrease.

Considering the considerable simplifications made in the model, the agreement with the 2D-MOT data is quite reasonable, both for the velocity distribution and the total flux. A similar vapor-cell based source has recently been proposed

by Vredenburg *et al.* [14]. Their proposal predicts a velocity distribution that peaks at much higher velocities than we observe. The transverse capture of atoms was ignored and only funneled atoms were taken into account. In contrast, our model shows that most of the flux in our experiment is a result of transverse capture, with only the high velocity tail arising from funneling. The reduced presence of atoms with high velocities is essentially due to the fact that the time available for transverse cooling falls off as l/v_z .

VII. CONCLUSION

The two-dimensional trapping geometry is very useful to produce slow atomic beams with low divergence out of a vapor cell. The continuous and transient character of the capture process reduces collisional loss from the background, so that high atomic flux can be achieved by increasing the background vapor pressure. Especially the 2D⁺-MOT employing additional cooling in the longitudinal direction yields a very high flux of almost 10^{10} atoms/s at 8 m/s and a narrow width of the velocity distribution of 3.3 m/s (FWHM). This was realized by means of comparatively low laser power. This source can be used for loading a magneto-optical trap, and thus provides an attractive alternative to loading from a Zeeman-slower or current double-MOT system. It may also find promising application in atom interferometry, atom optics, and atomic clocks based on fountains.

ACKNOWLEDGMENTS

This work is part of a research program of the Stichting voor Fundamenteel Onderzoek der Materie (FOM), which is a subsidiary of the Nederlandse Organisatie voor Wetenschappelijk Onderzoek (NWO). K.D. and M.W. are supported by a Marie Curie Research Training Grant of the Training and Mobility for Researchers (TMR) activity under the fourth European Community Framework Program for research and technological development. The research of R.S. has been made possible by support from the Royal Netherlands Academy of Arts and Sciences.

-
- [1] E. Riis, D. S. Weiss, K. A. Moler, and S. Chu, *Phys. Rev. Lett.* **64**, 1658 (1990).
 - [2] J. Nellesen, J. Werner, and W. Ertmer, *Opt. Commun.* **78**, 300 (1990).
 - [3] A. Scholz, M. Christ, D. Doll, J. Ludwig, and W. Ertmer, *Opt. Commun.* **111**, 155 (1994).
 - [4] M. H. Anderson, J. R. Ensher, M. R. Matthews, C. E. Wieman, and E. A. Cornell, *Science* **269**, 198 (1995).
 - [5] K. B. Davis, M.-O. Mewes, M. R. Andrews, N. J. van Druten, D. S. Durfee, D. M. Kurn, and W. Ketterle, *Phys. Rev. Lett.* **75**, 3969 (1995).
 - [6] C. C. Bradley, C. A. Sackett, J. J. Tollett, and R. G. Hulet, *Phys. Rev. Lett.* **75**, 1687 (1995).
 - [7] W. D. Phillips and H. Metcalf, *Phys. Rev. Lett.* **48**, 596 (1982).
 - [8] Z. T. Lu, K. L. Corwin, M. J. Renn, M. H. Anderson, E. A. Cornell, and C. E. Wieman, *Phys. Rev. Lett.* **77**, 3331 (1996).
 - [9] S. Weyers, E. Auccouturier, C. Valentin, and N. Dimarcq, *Opt. Commun.* **143**, 30 (1997).
 - [10] P. Berthoud, A. Joyet, G. Dudle, N. Sagna, and P. Thomann, *Europhys. Lett.* **75**, 1687 (1995).
 - [11] P. Julienne and J. Vigué, *Phys. Rev. A* **44**, 4464 (1991).
 - [12] A. M. Steane, M. Chowdhury, and C. J. Foot, *J. Opt. Soc. Am. B* **9**, 2142 (1992).
 - [13] K. Lindquist, M. Stephens, and C. Wieman, *Phys. Rev. A* **46**, 4082 (1992).
 - [14] E. J. D. Vredenburg, K. A. H. van Leeuwen, and H. C. W. Beijerinck, *Opt. Commun.* **147**, 375 (1998).